

Photopyroelectric Spectrum of MnO_2 Doped Bi_2O_3 - TiO_2 - ZnO Ceramic Combination

Zahid Rizwan¹, Azmi Zakaria^{2*}, W. Mahmood Mat Yunus², Mansor Hashim²
and Abdul Halim Shaari²

¹National Textile University, Sheikhpura road, Faisalabad (37610), Pakistan

²Department of Physics, Faculty of Science, Universiti Putra Malaysia,
43400 UPM, Serdang, Selangor, Malaysia

*E-mail: azmizak@fsas.upm.edu.my

ABSTRACT

Photopyroelectric spectroscopy is used to study the energy band-gap of the ceramic ($\text{ZnO} + 0.25 \text{Bi}_2\text{O}_3 + 0.25 \text{TiO}_2 + x \text{MnO}_2$), $x = 0 - 1.3$ mol%, sintered at isothermal temperature 1190 and 1270°C for 2 hours in air. The wavelength of incident light, modulated at 9 Hz, is kept in the range of 300 to 800 nm and the photopyroelectric spectrum with reference to the doping level is discussed. The energy band-gap is estimated from the plot $(ph\nu)^2$ vs $h\nu$ and is 2.80 eV for the samples without MnO_2 at both sintering temperatures. It decreases to 2.08 eV with a further increase of MnO_2 . The phase constitution is determined by XRD analysis. Microstructure and compositional analysis of the selected areas are analyzed using SEM and EDX. The maximum relative density, 91.4 %, and the grain size, 47 μm , were observed in this ceramics combination.

Keywords: Photopyroelectric, band gap, zinc oxide

INTRODUCTION

A white polycrystalline solid material Zinc Oxide (ZnO) crystallizes into a wurtzite structure. It is a n-type semiconductor material with a wide energy band-gap 3.2 eV (Gupta, 1990). It is widely used in the manufacturing of paints, rubber products, cosmetics, pharmaceuticals, floor covering, plastics, textiles, ointments, inks, soap, batteries, and also in electrical components such as piezoelectric transducers, phosphors, solar cell electrodes, blue laser diodes, gas sensors and varistors (Lin *et al.*, 1998; Look, 2001).

The exact role of many additives in the electronic structure of ZnO varistors is uncertain. ZnO based varistor is formed with small amounts of metal oxides such as Bi_2O_3 , Co_3O_4 , Cr_2O_3 , MnO , Sb_2O_3 and others. These additives are the main tools that are used to improve the non-linear response and the stability of ZnO varistor (Eda, 1989). It is necessary to get information of optical absorption of the ceramic ZnO doped with different metal oxides. This paper reports the use of photopyroelectric (PPE) spectrometer, a powerful non-radiative tool (Mandelis, 1984) to study optical properties and a discussion on the PPE spectroscopy of ZnO doped with $x\text{MnO}_2$ in the presence of 0.25 Bi_2O_3 , 0.25 TiO_2 .

Received : 11 January 2008

Accepted : 8 April 2008

* Corresponding Author

MATERIALS AND METHODS

ZnO (99.9 % purity) was doped with 0.25 Bi₂O₃, 0.25 TiO₂, and xMnO₂ where x = 0 - 1.3 mol%. Pre-sintered powders at 760°C in air for 2 hours were pressed at 800 kg cm⁻² to form disk shape samples. Disks were sintered at 1190 and 1270°C for 2 hours in air at the heating and cooling rate of 2.5°C min⁻¹. The density was measured by geometrical method. The mirror like polished samples were thermally etched for the microstructure analysis. Average grain size was determined by the grain boundary-crossing method. The disks of each sample were ground to make a fine powder for the PPE spectroscopic and XRD analysis. The XRD data were analyzed by using X'Pert High Score software for the identification of the crystalline phases. The measurement of PPE signal amplitude using the PPE spectrometer system to produce a PPE spectrum has been described elsewhere (Mandelis, 1984). In the present system, light beam was a 1 kW Xenon arc lamp that was kept in the range of 300 to 800 nm, mechanically chopped at 9 Hz, and scanned at 2 nm step size. The true PPE spectrum of the sample was obtained by normalizing PPE spectrum of sample with that of carbon black. Prior the PPE measurement, fine powder sample was ground in deionised water and a few drops of each mixture were dropped on 1.5 cm² aluminium foil and dried in air to form a thin sample layer about 12 µm thick on foil. The foil was placed in contact with PPE transducer (Tam and Coufal, 1983) using a very thin-layer of silver conductive grease. In determining the energy band-gap (E_g), it was assumed that the fundamental absorption edge of doped ZnO is due to the direct allowed transition. The optical absorption coefficient β varies with the excitation light energy $h\nu$ (Toyoda *et al.*, 1985) and is given by the expression, $(\beta h\nu)^2 = C (h\nu - E_g)$ near the band gap, where $h\nu$ is the photon energy, C is the constant independent of photon energy, and E_g is the direct allowed energy band-gap. The PPE signal intensity ρ is directly proportional to β , hence $(\rho h\nu)^2$ is related to $h\nu$ linearly. From the plot of $(\rho h\nu)^2$ versus $h\nu$, E_g is obtained by extrapolating the linear fitted region that crosses photon energy axis.

RESULTS AND DISCUSSION

The XRD analysis, *Fig. 1*, of the ceramic shows that the major phase is hexagonal ZnO and the secondary phase is Bi₄Ti₃O₁₂ (ref. code 00-12-0213) developed in all samples at all doping levels and temperatures. Few peaks of Bi₂O₃ (ref. code 00-018-0244), Mn₂TiO₄ (ref. code 00-016-0241) were also observed in the pattern. Relative density increases from 88.7, 89.3% to 91.4, 90.6% with the increased of MnO₂ for 1190 and 1270 °C sintering temperatures, respectively, *Fig. 2*. It is slightly higher at lower sintering temperature. Grain size increased from 22.5, 24.8 to 46.3, 47.1 µm with the increase of MnO₂ for the sintering temperature 1190, 1270 °C, respectively, as depicted in *Fig. 3*. This indicates that the MnO₂ acts as a grain enhancer even in the presence of the other grain enhancers 0.25 Bi₂O₃ and 0.25 TiO₂ which are present in the ceramic.

From SEM and EDX, *Fig. 5*, it shows that Bi₂O₃ is segregated at grain boundaries as well as at triple point junctions. Some patches of the Zn, Ti, Mn additives were found on the grain surface of the grains. These are due to the in-homogeneous mixture of the ceramics. The energy band-gap (E_g) of the ceramics is reduced from 3.2 eV (pure ZnO) to 2.80 ± 0.01 eV at the 0 mol% of MnO₂ for 1190 and 1270°C sintering temperatures, *Fig. 4*. The reduction of 0.40 ± 0.01 eV is due to the interface states produced by the combined effect of Bi₂O₃ and TiO₂ additives at the two sintering temperatures. The energy band-gap is drastically decreased down to 2.24, 2.22 eV for sintering temperatures

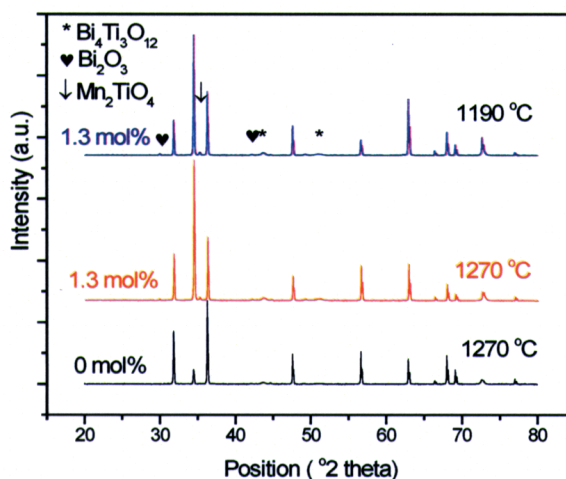


Fig. 1: XRD pattern at different doping level of MnO_2

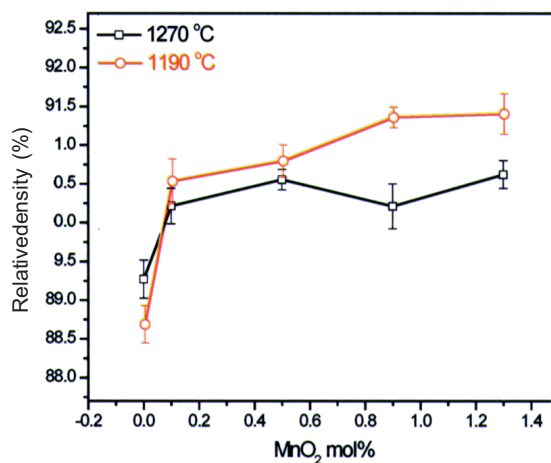


Fig. 2: Variation of density with MnO_2

1190, 1270 °C, respectively, at 0.1 mol% of MnO_2 . This rapid decrease is about 0.58 eV which is due to the growth of interface states in the grain interior and also in the grain boundaries. With further amount of MnO_2 addition into the ceramic, E_g is found continuously decreasing down to 2.08 eV at 1.3 mol% of MnO_2 at both sintering temperatures. This small decrease, about 0.14 eV, is due to the growth of interface states with the addition of MnO_2 (Toyoda and Shimamoto, 1998). The overall value of E_g is slightly lower at the higher sintering temperature at all doping levels. This indicates that the increase in the sintering temperature is not effective at decreasing the value of E_g . It is observed that the decrease in the E_g due to the combined effect of the 0.25 Bi_2O_3 and 0.25 TiO_2 additives at both sintering temperatures is about 0.40 eV but the decrease in

E_g is about 0.58 eV only at 0.1 mol% MnO_2 . Ionic radius of Mn ion (0.53 \AA) is smaller than the ionic radius of Zn (0.74 \AA) (Yoshikazu *et al.*, 2002; Dow and Redfield, 1972; Urbach, 1953) so Mn ions substitutes the Zn ions and contributes to further increase of interface states hence further decrease of E_g .

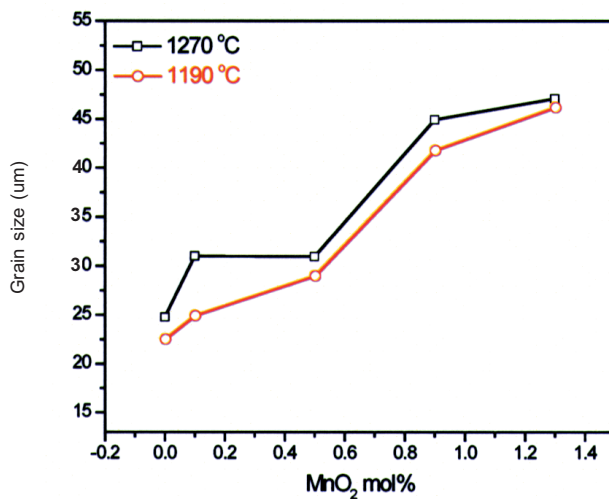


Fig. 3: Variation of grain size with MnO_2

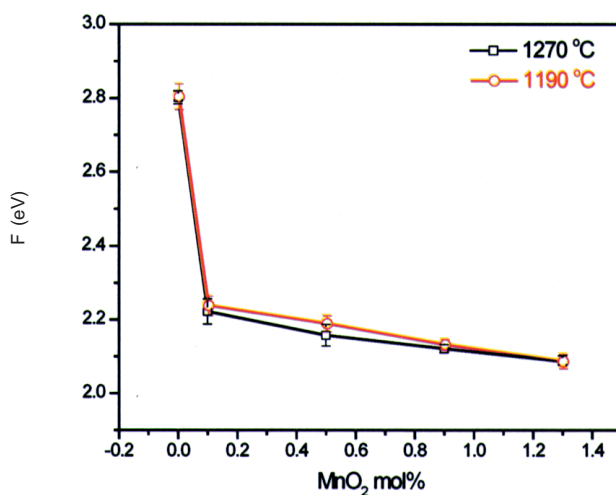


Fig. 4: Dependence of E_g on MnO_2

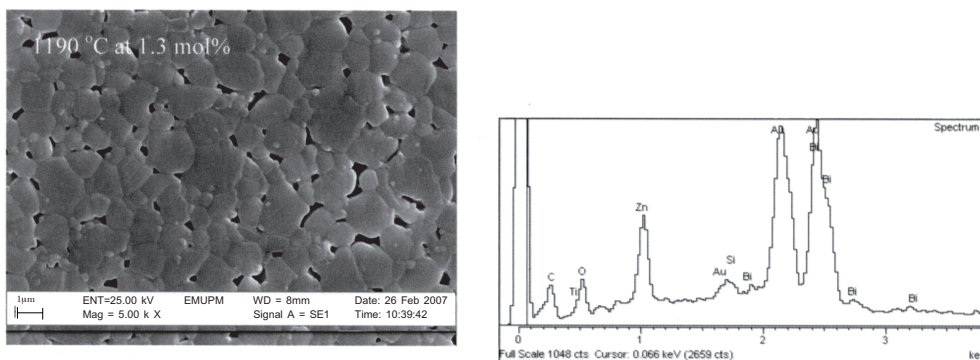


Fig. 5: SEM micrograph for 1.3 mol% and EDX spectrum at the grain boundary for 0.1 mol% MnO_2 at 1190 °C sintering temperature

CONCLUSIONS

Spectroscopic results are discussed with the doping of MnO_2 and found that the MnO_2 acts as a grain enhancer. Both Bi_2O_3 and TiO_2 reduce the energy band-gap but MnO_2 does contribute more prominently.

ACKNOWLEDGEMENTS

Thanks to MOSTI for the financial assistance (Grant FRGS No. 01-01-07-139FR) for this research.

REFERENCES

- DOW, J.D. and REDFIELD, D. (1972). Towards a unified theory of Urbach's rule and exponential absorption edge. *Phys. Rev.*, *B5*, 594.
- EDA, K. (1989). Zinc oxide varistors. *IEEE Elect. Insul. Mag.*, *5*, 28-41.
- GUPTA, T.K. (1990). Application of zinc oxide varistors. *J. Am. Ceram. Soc.*, *73*(7), 1817-40.
- LIN, H.M., TZENG, S.J., HSIAU, P.J. and TSAI, W.L. (1998). Electrode effects on gas sensing properties of nanocrystalline zinc oxide. *Nanostruct. Mater.*, *12*, 465- 77.
- LOOK, D.C. (2001). Recent advances in ZnO materials and devices. *Mat. Sci. Eng. B*, *80*, 383-87.
- MANDELIS, A. (1984). Frequency-domain photopyroelectric spectroscopy of condensed phases (PPES): A new, simple and powerful spectroscopic technique. *Chem. Phys. Lett.*, *108*, 388-92.
- TAM, A.C. and COUFAL, H. (1983). Photoacoustic generation and detection of 10-ns acoustic pulses in solids. *Appl. Phys. Lett.*, *42*, 33-5.
- TOYODA, T., NAKANISHI, H., ENDO, S., and IRIE, T. (1985). Fundamental absorption edge in semiconductor CdInGaS_4 at high temperatures. *J. Phys. D Appl. Phys.*, *18*, 747-51.
- TOYODA, T. and SHIMAMOTO, S. (1998). Effect of Bi_2O_3 impurities in ceramic ZnO on photoacoustic spectra and current-voltage spectra. *Jpn. J. Appl. Phys.*, *37*, 2827-31.

YOSHIKAZU, S., YASUHIRO, O., TOSHIO, K. and JUN, M. (2002). Evaluation of Sb_2O_3 -doped ZnO varistors by photoacoustic spectroscopy. *Jpn. J. Appl. Phys.*, 41, 3379-82.

URBACH, F. (1953). The long-wavelength edge of photographic sensitivity end of the electronic absorption of solids. *Phys. Rev.*, 92, 1324.